GROUND EXPERIMENT AND NUMRICAL SIMULATION OF SPACECRAFT ARCING IN AMBIENT PLASMA ENVIRONMENTS

Takahisa Masuyama
Department of Mechanical Science and Bioengineering
Graduate School of Engineering Science, Osaka University
1-3, Machikaneyama, Toyonaka, Osaka 560-8531, Japan
Phone: +81-6-6850-6178
Fax: +81-6-6850-6179
E-mail: tahara@me.es.osaka-u.ac.jp

Masato Nagata
Tatsuo Onishi
Hirokazu Tahara
Takao Yoshikawa
Osaka University, Japan

Abstract

In the future, LEO spacecraft will be larger and higher powered. Because of the balance of leakage currents through ambient space plasma, their main conductive body will have a higher negative potential without plasma contactor operation. When spacecraft operate with a higher voltage, more intensive arcing is suspected to occur on the surface. In this study, ground-based experiment and Direct-Simulation-Monte-Carlo Particle-In-Cell plasma simulation were carried out to understand the arcing phenomenon and to examine influences of ambient space plasma on the arcing process. Simulating plasmas were generated by electron cyclotron resonance discharge. When arcing occurred on negatively-biased anodized aluminum sample (AAS) plates in the plasma environment, the time variations in arc current and bias voltage were measured. Arc spot diameter was also measured. The experimental results showed that both the peak arc current and the total charge emitted by arcing increased with initial charging voltage and neutral particle number density. The diameter of arc spots increased with initial charging voltage although it was almost constant regardless of neutral particle density. The calculated results showed that neutral particles in addition to charged particles around spacecraft played an important role in expansion of arc plasma causing the arcing characteristics. Accordingly, high voltage operation of LEO spacecraft might bring drastic degradation of AAS by arcing depending on ambient plasma conditions.

Introduction

Spacecraft are in a severe environment in space. Their surfaces are exposed to energetic and reactive particles, such as electrons, ions, protons and oxygen atoms and ultraviolet light, including particles exhausted from plasma thrusters, during space missions. The environmental effect plays a crucial role in determining the spacecraft's reliability and lifetime [1]. Although the number density of ions such as oxygen and nitrogen is smaller than that of atomic oxygen in LEO, electrostatic interactions between the surface materials and the ambient plasma, such as negative or positive sheath creation, and charging and arcing phenomena, frequently occur. The ions are accelerated in a negative potential sheath on a solar array, and the current generated by the solar array is leaked by impact of the ions; the solar array is still degraded by sputtering and arcing due to the collected ions [2],[3]. Accordingly, the environmental factors cause changes of chemical structures of spacecraft materials and their optical and/or electrical properties [4],[5]. In GEO satellites, it is well-known that the electrical breakdown of negative charging on their insulating surfaces causes intensive damages in

the systems. In plasma contactor operations, the negative charging is expected to be mitigated by ions attracted from the plasma, resulting in surface degradation as well as in cases with high voltage solar arrays [6]-[8]. The mechanism of the material degradation, the structure of electrical sheaths, and the charging and arcing processes must be understood.

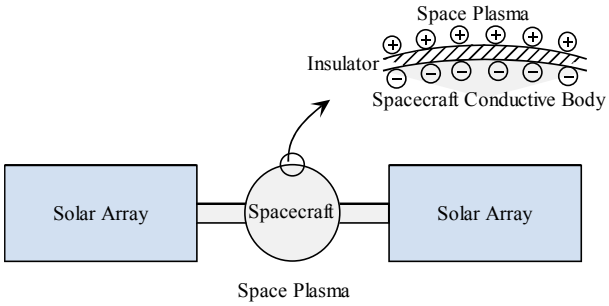

Figure 1. Feature of charging on spacecraft surface insulators.

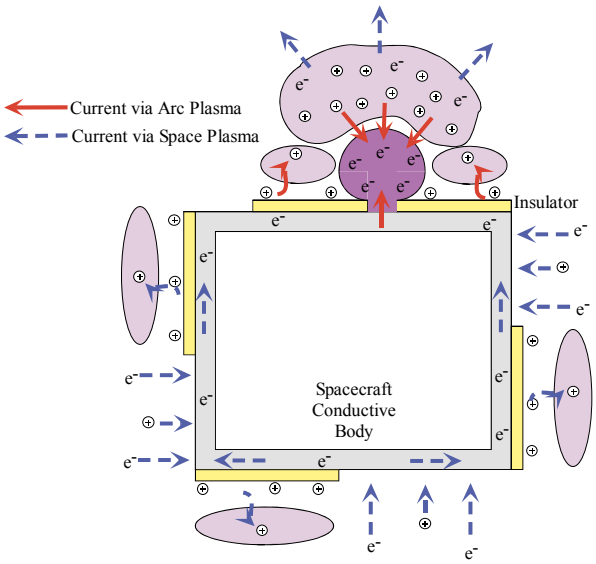

(a) Spacecraft body.

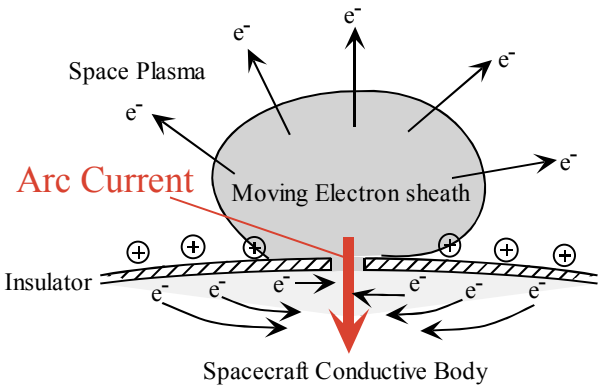

(b) Near arc spot.

Figure 2. Current paths for arcing on surface insulator between spacecraft conductive body and space plasma.

In Osaka University, the structure of an ion sheath created around a high voltage solar array and the degradation of surface materials near the array due to high energy ion bombardment have been investigated [2],[3],[5]. The mitigation of negative charging by plasma flow, i.e. the feature of plasma contactor operations, has also been studied [6]-[8].

In the future, LEO spacecraft will be larger and higher powered. Because of the balance of leakage currents through ambient space plasma, their main conductive body will have a higher negative potential without plasma contactor operation. When spacecraft operate with a higher voltage, more intensive arcing is suspected to occur on the spacecraft surface. In this study, ground-based experiment is carried out to understand this phenomenon and to examine influences of ambient space plasma on the arcing process. Simulating plasmas are generated by electron cyclotron resonance (ECR) discharge. Arcing characteristics of negatively-biased anodized aluminum sample (AAS) plates in the plasma environment are investigated. When arcing occurs on the plate, the time variations in arc current and bias voltage are measured. Arc spot diameter is also measured. Furthermore, Direct-Simulation-Monte-Carlo Particle-In-Cell (DSMC-PIC) plasma simulation is conducted to understand features of plasma expanding from an arc spot on a spacecraft surface into the ambient plasma just after arcing.

Hazard of Drastic Destruction of Spacecraft Surface Materials by Arcing in Plasma Environment

In general, the spacecraft conductive body, as shown in Fig.1, has a negative potential, near solar array voltage, on potential of space plasma. It is called absolute negative charging. Then, positive charging occurs on an insulator of the spacecraft surface. The large insulator works as a capacitor with a high capacitance. As shown in Fig.2(a), if electric breakdown occurs between the spacecraft conductive body and space plasma, i.e. destruction of the insulator by arcing, arc currents flow through several paths until neutralization of charge is finished. As a result, the arc current flowing from space plasma to the arc point of the spacecraft conductive body, as shown in Fig.2(b), is very high because of the high capacitance of the insulator. The arcing is suspected to intensively degrade insulator materials of spacecraft surface, specially with a high voltage solar array. Furthermore, the arcing characteristics are considered to depend on feature of space plasmas near spacecraft surface because interaction between electrons extracted from the arc spot and the ambient space plasma is expected to occur. Intensive arcing is suspected to occur in some ambient plasma environment.

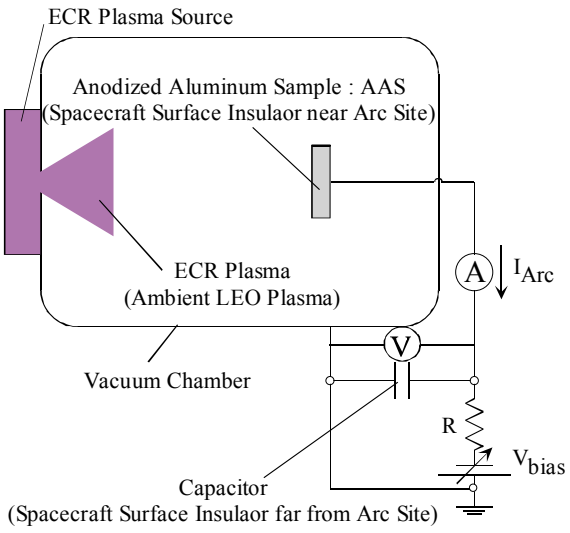

Figure 3. Experimental system for arcing of negatively-biased anodized aluminum sample (AAS) plates in plasma environment.

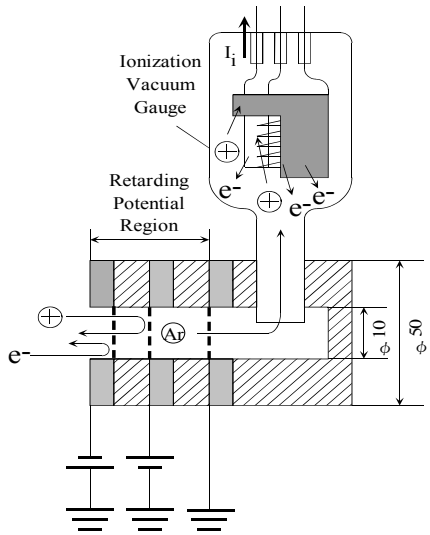

Figure 4. Configuration of retarding-potential-type neutral particle probe.

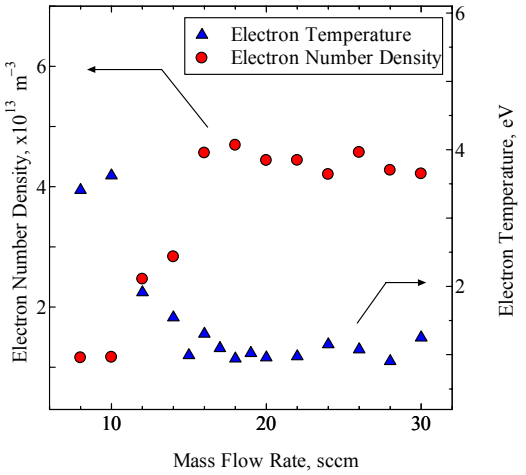

(a) Electron number density and electron temperature.

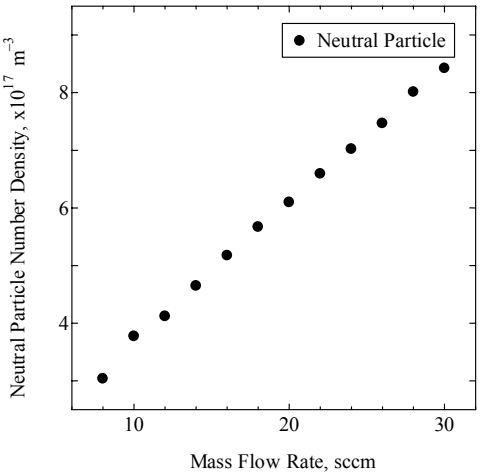

(b) Neutral particle number density.

Figure 5. Plasma properties measured at center of AAS plate located 660 mm downstream from plasma source exit. The microwave input power is 300 W.

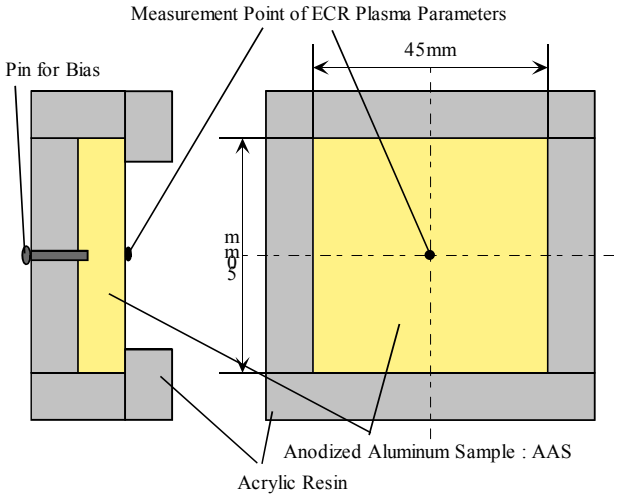

Figure 6. Configuration of sample holder of negatively-biased AAS plates.

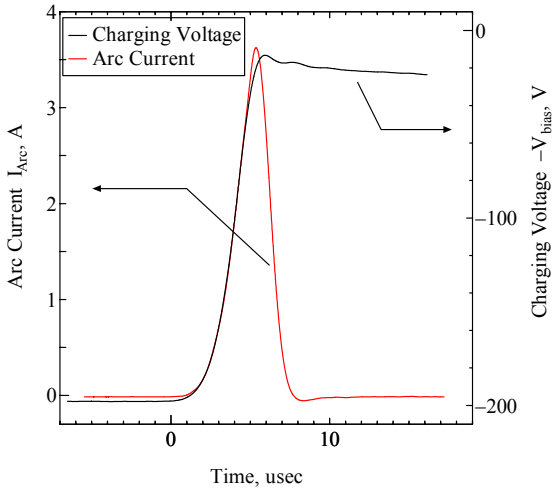

Figure 7. Typical time variations in charging voltage and arc current for arcing of AAS plate in plasma environment.

Experimental Apparatus

Figure 3 shows the experimental system for arcing of negatively-biased anodized aluminum sample (AAS) plates in plasma environment. The experimental facility developed in Osaka University mainly consists of a vacuum tank, a vacuum pump system, a plasma source and an AAS plate [9]. The electron cyclotron resonance (ECR) plasma source is set on a flange of the large stainless vacuum tank 0.7 m in diameter x 1.5 m long. The main vacuum pump is an oil-free turbo-molecular pump with a high pumping speed of 5 m^3/s. The tank pressure is kept some 10^{-3} Pa during all experiments.

Argon plasmas simulating spacecraft ambient plasma are produced by ECR discharge. Microwaves of maximum 1 kW and 2.45 GHz are introduced into the ECR discharge chamber. An orifice is set to the downstream exit of the discharge chamber to produce a low-density plasma.

Electron number density and electron temperature are measured with a Langmuir probe. Neutral particle number density is also measured by a retarding-potential-type neutral particle probe shown in Fig.4.

Figure 5 shows the plasma properties measured at the center of the AAS plate located 660 mm downstream from the plasma source exit. The microwave input power is 300 W. When the argon flow rate increases from 8 sccm, the electron number density increases from $1.2x10^{13}m^{-3}$ and the electron temperature decreases from 4.0 eV. Over a flow rate of 16 sccm, they saturate with $4.5x10^{13}$ m^{-3} and 1 eV, respectively. The neutral particle number density linearly increases from $3.0x10^{17}m^{-3}$ with a flow rate of 8 sccm to $8.5x10^{17}m^{-3}$ with 30 sccm.

As shown in Fig.6, an AAS plate 50 mm x 50 mm square is used in this experiment. The plate made from Al2017 is prepared with MIL-A-8625-TYPE I, and the anodized layer is 1.3 um thick as well as those of Japanese Experimental Module in International Space Station. To simulate large surface area of spacecraft, a capacitor is connected between the AAS and a vacuum chamber, i.e. the ground. When arcing occurs, the time variations in arc current and charging voltage are measured. The diameter of arc spots also is measured.

Experimental Results and Discussion

Figures 7 and 8 show typical time variations in charging voltage and arc current, and a photograph of arc spot, respectively, for arcing of an AAS plate. The charging voltage rapidly changes from an initial charging voltage to zero, and then the arc current also rapidly changes up and down. The peak arc current is the order of ampere. As shown in Fig.8, a large hole with some ten um is created by arcing. The anodized layer is eroded, and the main aluminum part appears. Accordingly, degradation of material properties by arcing is suspected.

Figure 9 shows the time variations in charging voltage and arc current, and the characteristics of peak arc current, arcing impedance, total emitted charge, total emitted charge ratio and arc spot diameter, dependent on initial charging voltage at constant plasma parameters of neutral particle density, plasma density and electron temperature of $3.0x10^{17}$ m^{-3}, $1.2x10^{13}$ m^{-3} and 4 eV. The arc impedance is defined as a value of peak arc current divided into initial charging voltage. The total emitted charge is a value integrating arc current in time. Since the value does not equal the charge initially stored in the capacitor, the total emitted charge ratio can be defined as a ratio of total emitted charge to initial charge in the capacitor. The charging voltage, as shown in Fig.9(a), rapidly approaches zero from each initial charging voltage. At -400 and -500 V, the charging voltage transiently increases above zero. This is considered because a large amount of ions created by intensive ionization of an eroded and evaporated AAS, and/or neutral particles in the ambient plasma enters the arc spot. The arc current, as shown in Fig.9(b), rapidly increases and has a peak; then decreases. The peak arc current and the arc impedance, as shown in Figs.9(c) and 9(d), increases and decreases, respectively, with an increase in initial charging voltage from 100 to 500 V, and the duration time of arcing becomes short. A higher density plasma is considered to be created with increasing initial charging voltage. As a result, both the total emitted charge and the total emitted charge ratio, as shown in Fig.9(e), linearly increase with initial charging voltage. Because the total emitted charge ratio above 1.0 is achieved, an additional current flows from the ambient plasma. The additional current is considered to be an ion current created by intensive ionization in the ambient plasma as mentioned above. The diameter of arc spots, as shown in Fig.9(f), is almost constant at charging voltages up to 350 V and increases with above it. This shows that a large volume of the AAS is eroded and evaporated with a high initial charging voltage, resulting in creation of a dense plasma around the arc spot by intensive ionization.

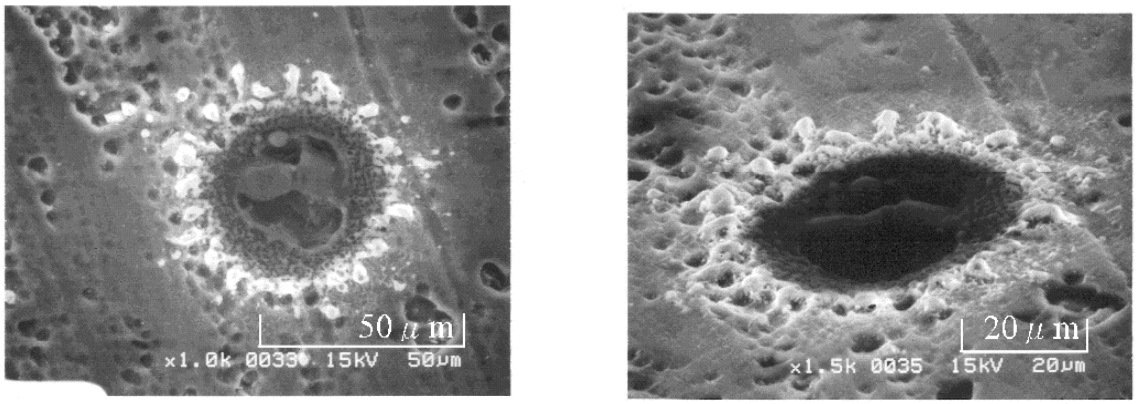

(a) Front. (b) Sideways.

Figure 8. Typical photograph of arc spot for arcing of AAS plate.

Figure 10 shows the time variations in charging voltage and arc current, and the characteristics of peak arc current, arcing impedance, total emitted charge, total emitted charge ratio and arc spot diameter, dependent on neutral particle number density at plasma parameters of 1.2-4.5x10^{13} m^{-3}, 1-4 eV and constant initial charging voltage of -200 V. Both the charging voltage and the arc current, as shown in Figs.10(a) and 10(b), show rapider and more intensive changes with increasing neutral particle density. This is considered because of ionization enhanced with high-density neutral particles as well as cases with high initial charging voltages shown in Fig.9. The characteristics of peak arc current, arcing impedance, total emitted charge and total emitted charge ratio agree with those of charging voltage and arc current. The total emitted charge ratio also reaches above 1.0 at high neutral particle densities. On the other hand, the arc spot diameter, as shown in Fig.10(f), is almost constant regardless of neutral particle density because the energy stored in the capacitor is constant.

Plasma Particle Simulation

DSMC-PIC simulation of electron-flow-induced plasma expandingfrom spacecraft surface into ambient plasma environment

Direct-Simulation-Monte-Carlo Particle-In-Cell (DSMC-PIC) plasma simulation is carried out to understand features of plasma expanding from an arc spot on a spacecraft surface into the ambient plasma just after arcing. Figure 11 shows the two-dimensional calculation model. Electrons are injected from an arc spot on Y-axis corresponding to a spacecraft insulator surface. The width of the arc spot is assumed to be 2.36x10^{-5} m from the experimental data. As shown in Fig.11(b), the electrical potential of the arc spot is linearly applied in time, and then the constant electron charge, which is the charge initially stored in the capacitor divided by the arc duration time of about 10 us, is introduced in time from the arc spot. In the ambient plasma environment, there exist electrons, ions and neutrals. Both elastic and ionization collisions between electrons and neutrals are considered. Both electrons and ions move electrostatically. The kinetic equations of electron and ion, and Poisson's equation are governing ones, and Leap Flog scheme and Successive-Over-Relaxation method are used for their integrations.

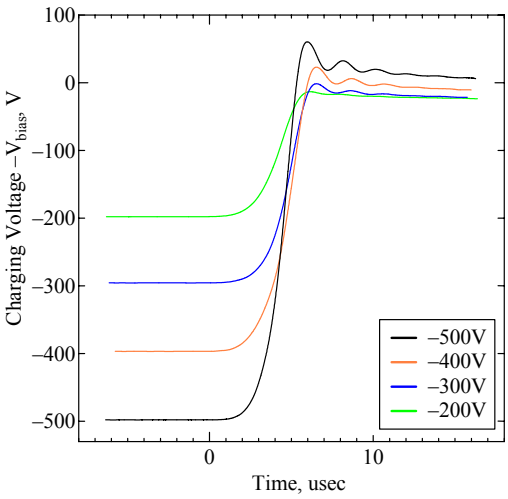

(a) Time variation in charging voltage.

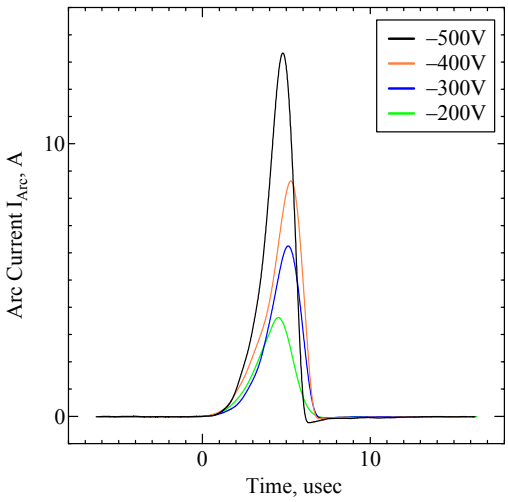

(b) Time variation in arc current.

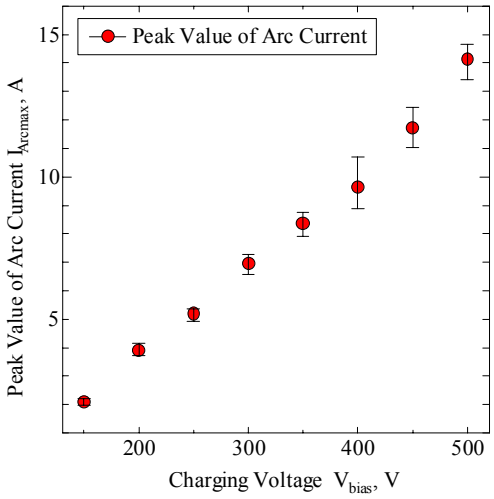

(c) Peak arc current.

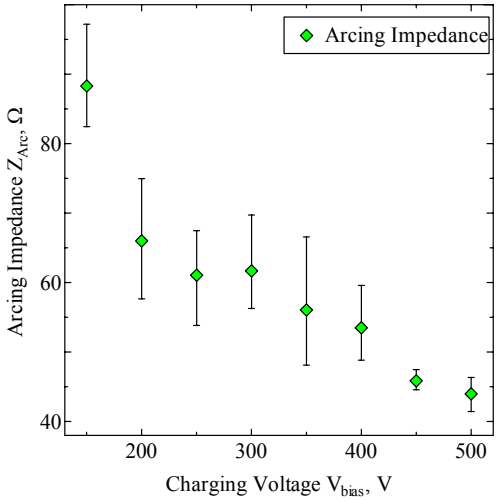

(d) Arcing impedance.

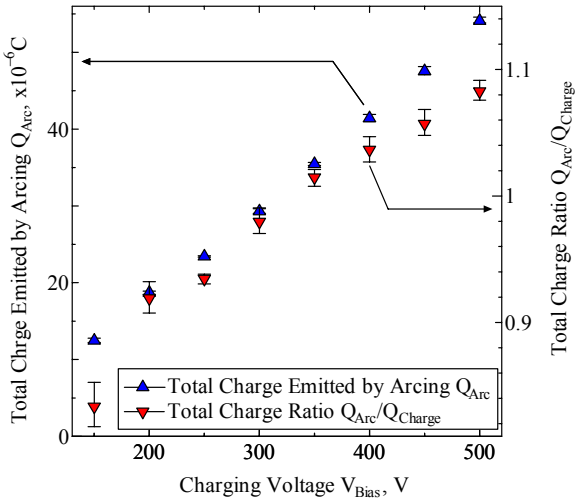

(e) Total emitted charge and total emitted charge ratio.

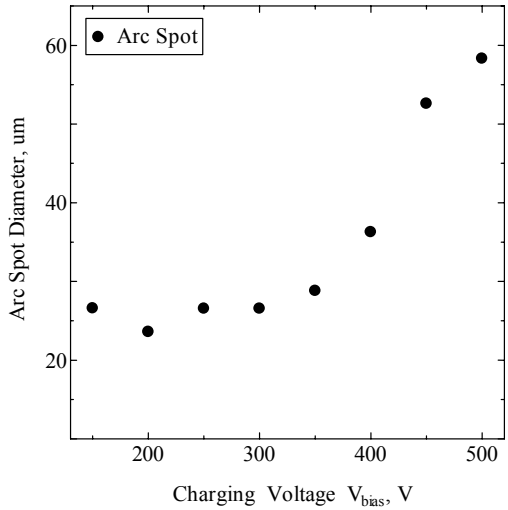

(f) Arc spot diameter.

Figure 9. Arcing characteristics dependent on initial charging voltage at constant plasma parameters of neutral particle density, plasma density and electron temperature of 3.0×10^{17} m^{-3}, 1.2×10^{13} m^{-3} and 4 eV.

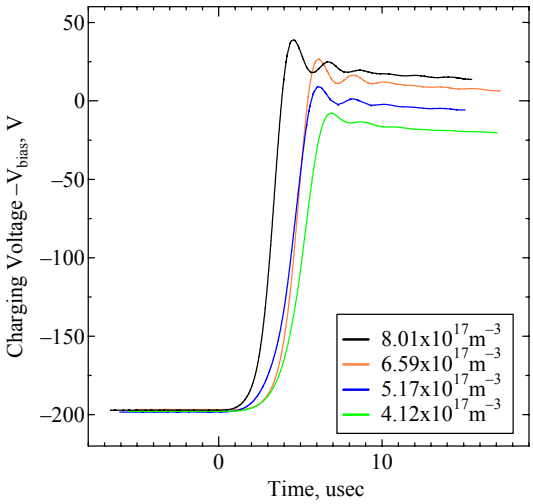

(a) Time variation in charging voltage.

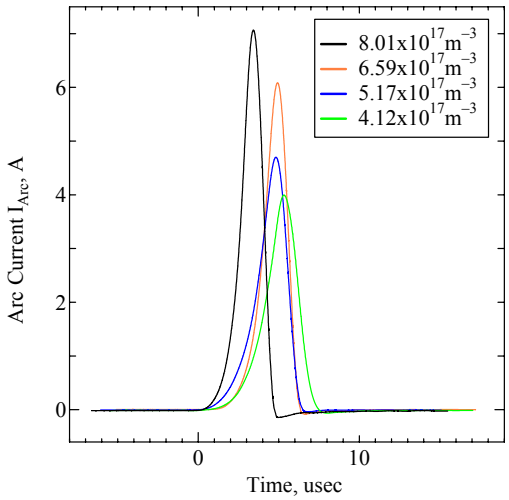

(b) Time variation in arc current.

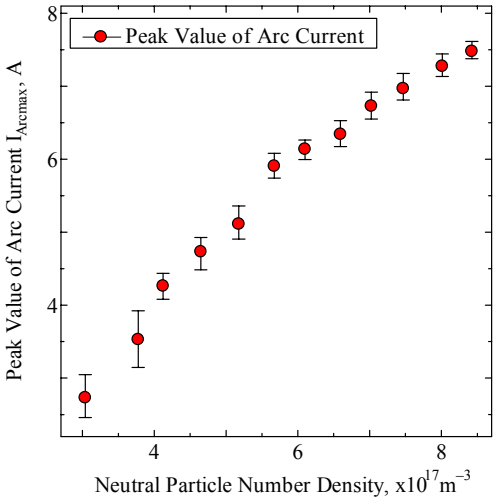

(c) Peak arc current.

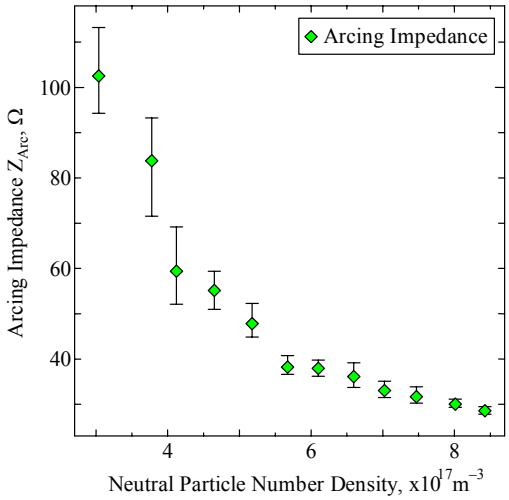

(d) Arcing impedance.

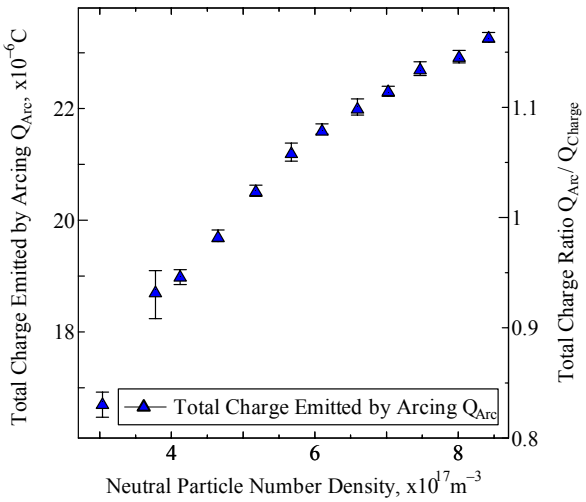

(e) Total emitted charge and total emitted charge ratio.

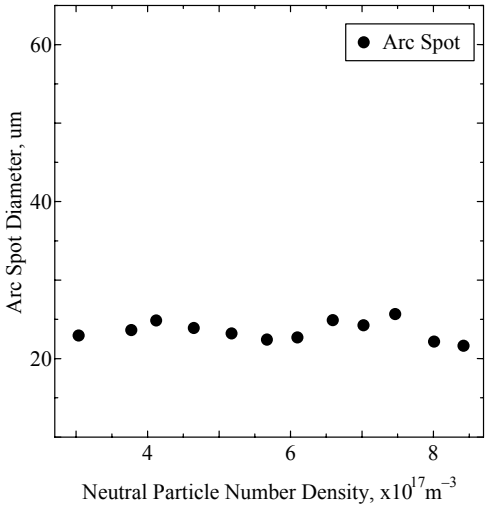

(f) Arc spot diameter.

Figure 10. Arcing characteristics dependent on neutral particle number density at plasma parameters of 1.2-4.5x10^{13} m^{-3}, 1-4 eV and constant initial charging voltage of -200 V.

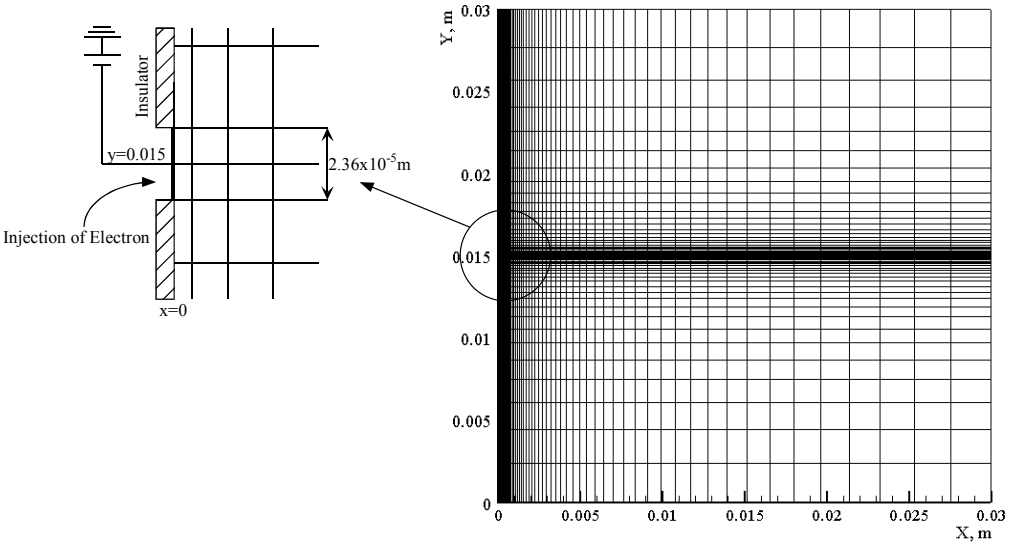

(a) Calculation domain.

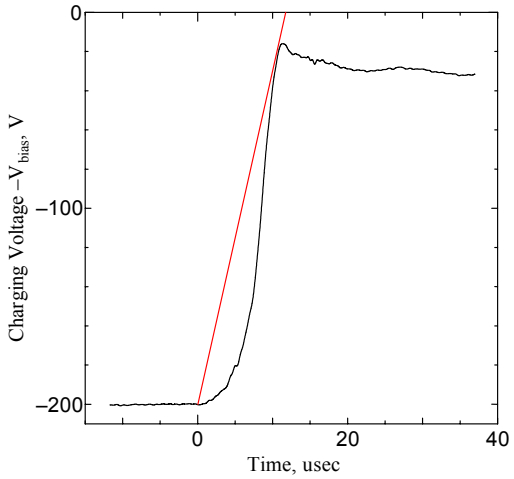

(b) Time variation in voltage applied at arc spot for calculation.

Figure 11. Two-dimensional calculation model of Direct-Simulation-Monte-Carlo Particle-In-Cell (DSMC-PIC) simulation of electron-flow-induced plasma expanding from spacecraft surface into ambient plasma environment

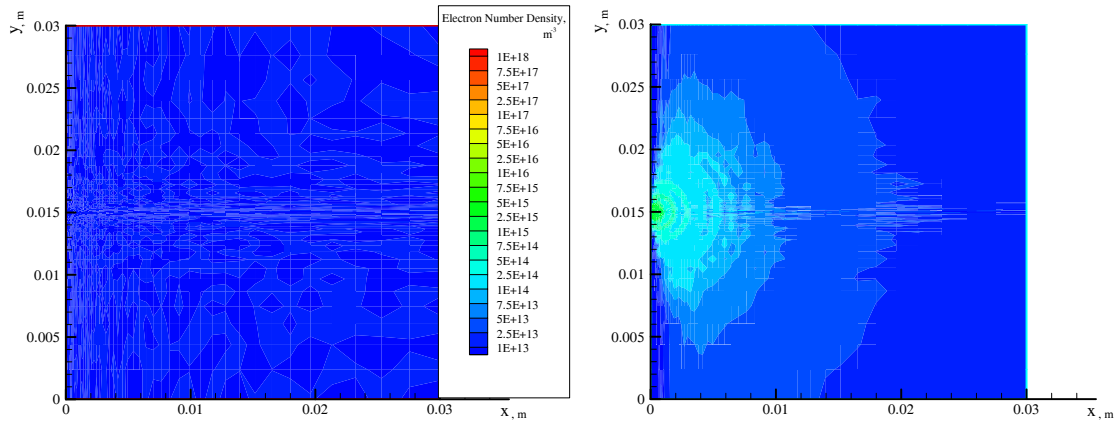

(a) 0 us.

(d) 6 us.

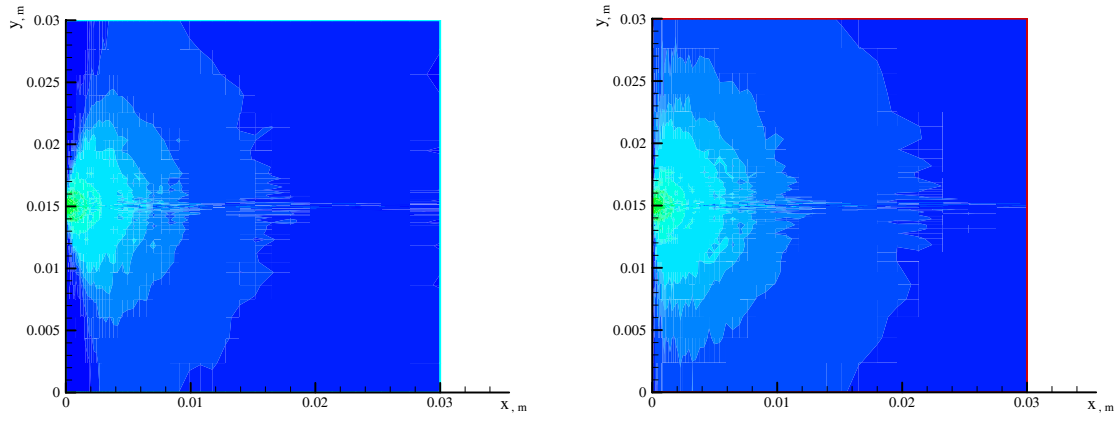

(b) 2 us.

(e) 8 us.

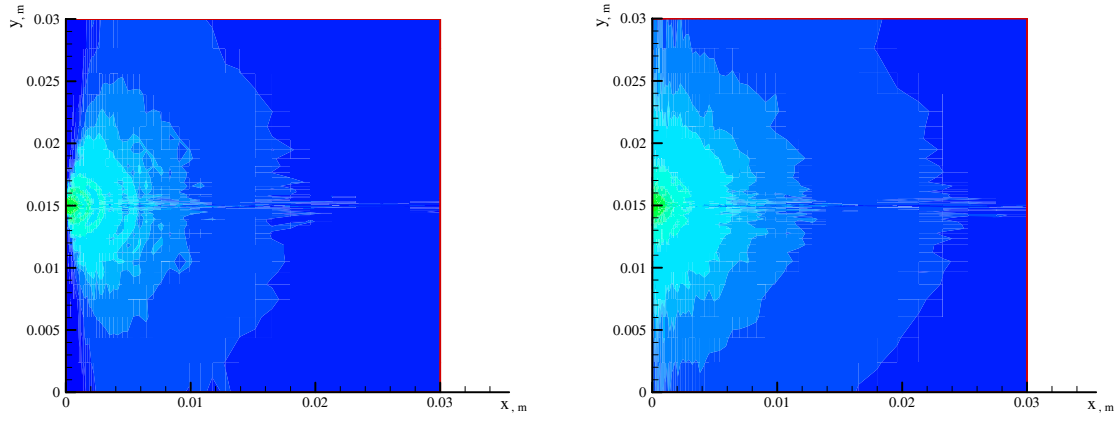

(c) 4 us.

(f) 10 us.

Figure 12. Time variation of pattern of electron number density at initial charging potential of -200 V with ambient plasma condition of plasma density 1.0×10^{13} m^{-3} and neutral particle density 1.0×10^{18} m^{-3}.

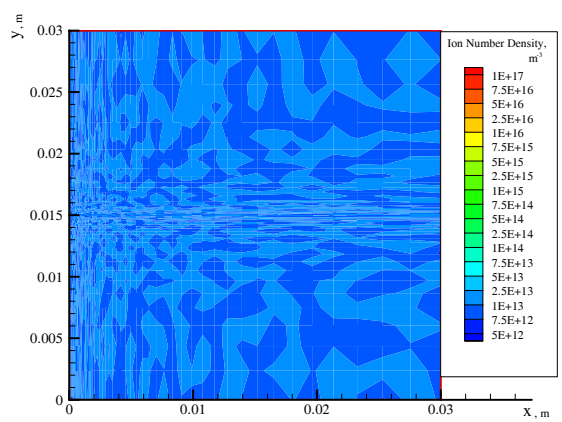

(a) 0 us.

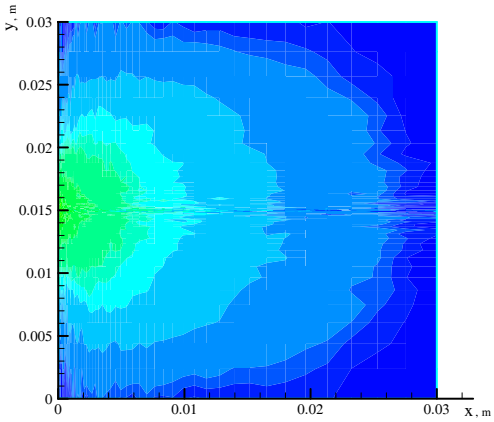

(d) 6 us.

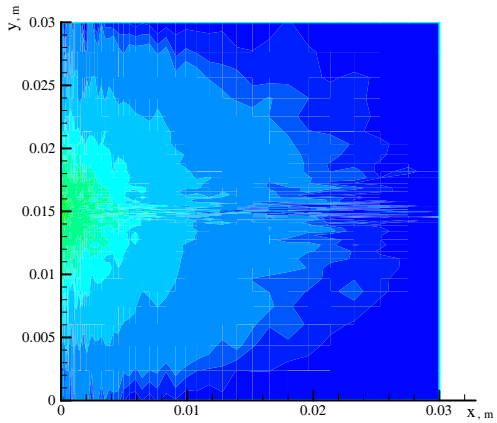

(b) 2 us.

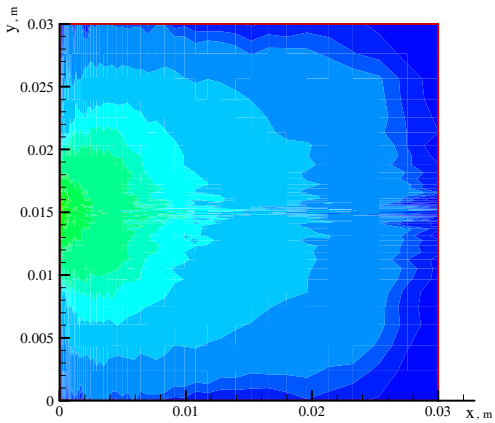

(e) 8 us.

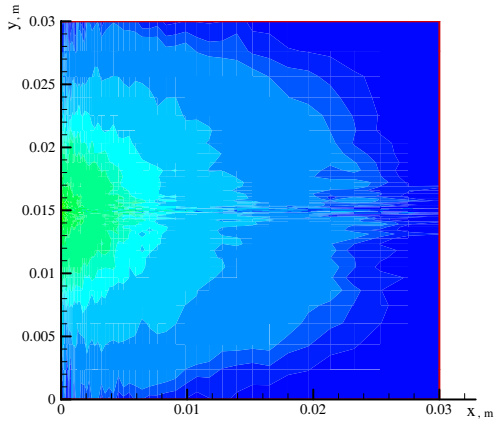

(c) 4 us.

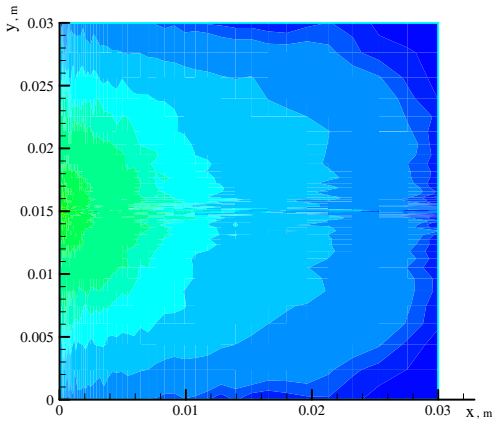

(f) 10 us.

Figure 13. Time variation of pattern of ion number density at initial charging potential of -200 V with ambient plasma condition of plasma density 1.0×10^{13} m^{-3} and neutral particle density 1.0×10^{18} m^{-3}.

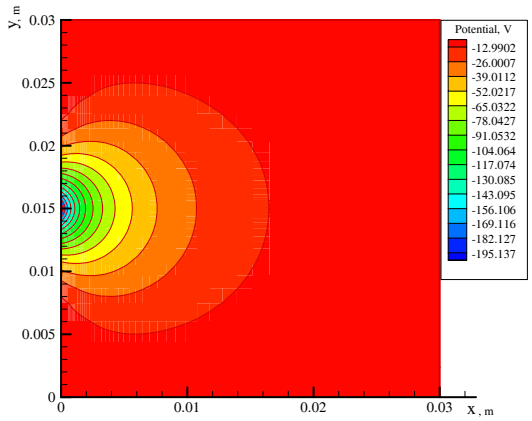

(a) 0 us.

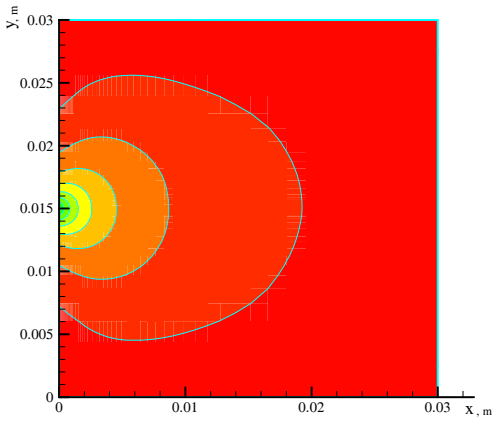

(d) 6 us.

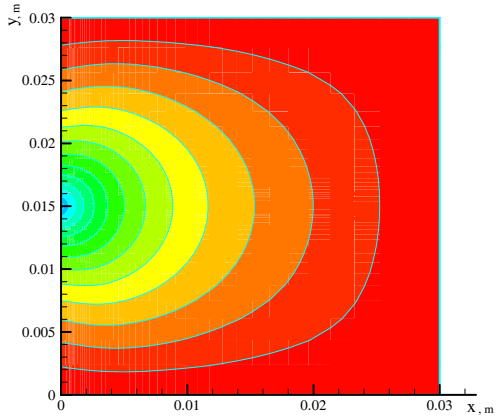

(b) 2 us.

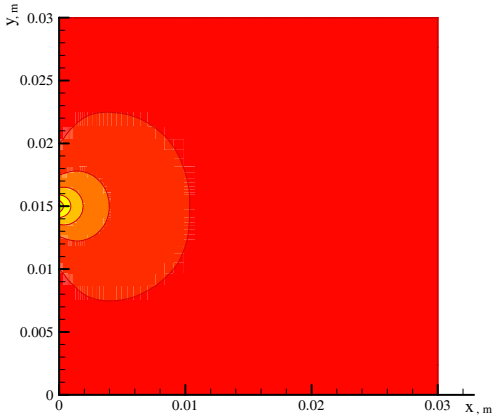

(e) 8 us.

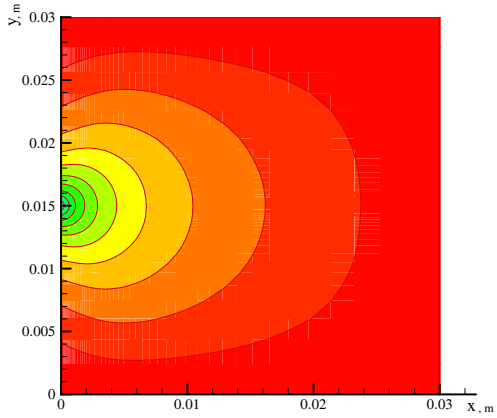

(c) 4 us.

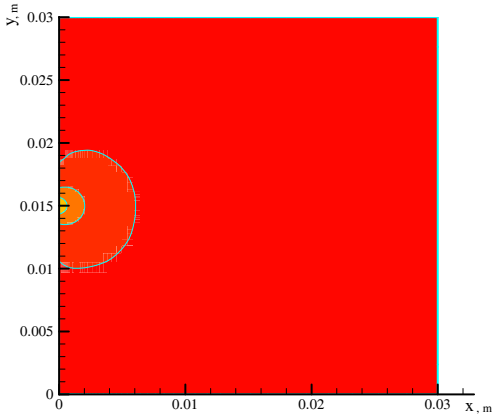

(f) 10 us.

Figure 14. Time variation of pattern of plasma potential at initial charging potential of -200 V with ambient plasma condition of plasma density 1.0×10^{13} m^{-3} and neutral particle density 1.0×10^{18} m^{-3}.

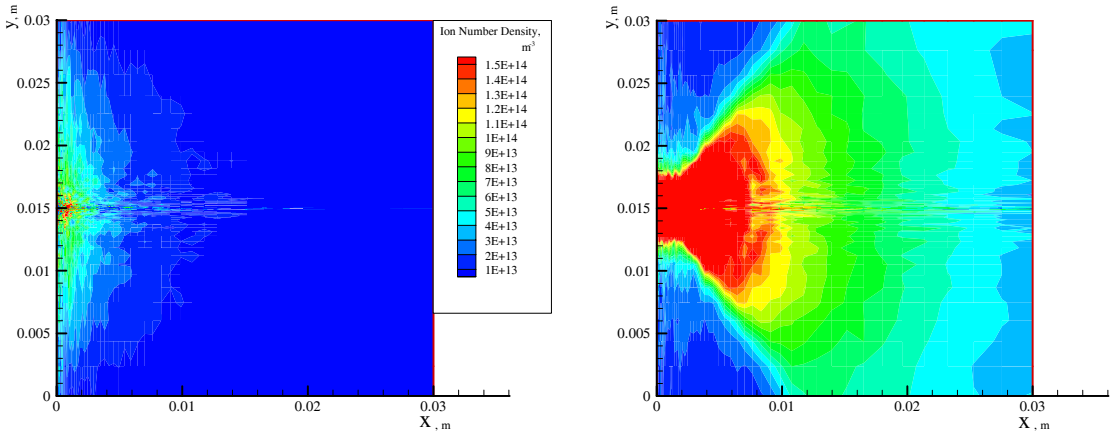

(a) Neutral density: 1.0×10^{17} m^{-3}. (b) Neutral density: 1.0×10^{19} m^{-3}.

Figure 15. Patterns of ion number density dependent on neutral particle number density at 8 us after start of arcing.

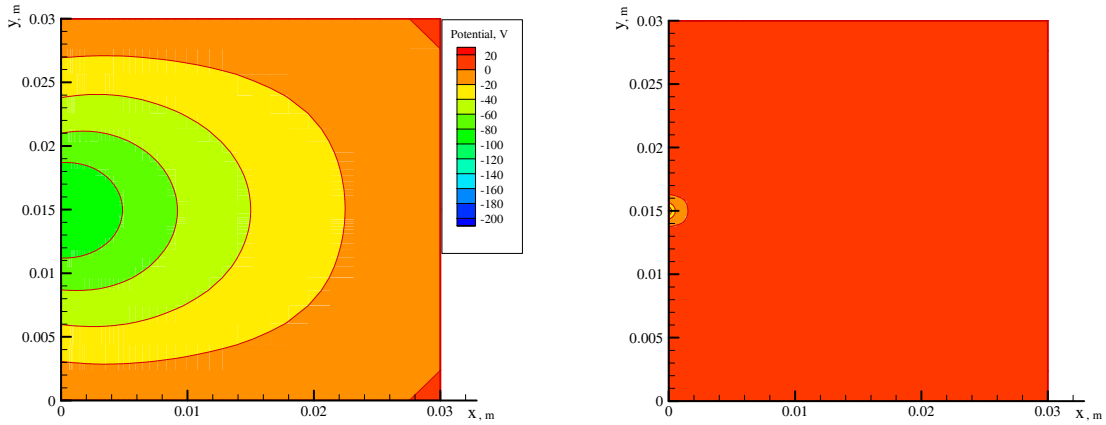

(a) Neutral density: 1.0×10^{17} m^{-3}. (b) Neutral density: 1.0×10^{19} m^{-3}.

Figure 16. Patterns of plasma potential dependent on neutral particle number density at 8 us after start of arcing.

Calculated results and discussion

Figures 12-14 show the time variations of patterns of electron number density, ion number density and plasma potential at an initial charging potential of -200 V with an ambient plasma condition of plasma density 1.0×10^{13} m^{-3} and neutral particle density 1.0×10^{18} m^{-3}. Electrons injected from the arc spot are rapidly expanding. The ion number density increases toward the arc spot. This is mainly considered because of intensive ionization due to high-energy electrons near the arc spot and because of ions electrostatically attracted toward the arc spot. The plasma potential pattern agrees with those of electron and ion densities. From the plasma potential pattern shown in Fig.14, the electric field is very high near the arc spot and decreases outwards. The spatial change in plasma potential expands up to 2 us because of drastic phenomena just after start of arcing, i.e. ionization, and rapid motions of electrons and ions, and after that the area becomes small.

Figures 15 and 16 show the patterns of ion density and plasma potential dependent on neutral particle number density at 8 us after start of arcing. There exists a high ion density region in front of the arc spot. When the neutral particle density increases, the area becomes large because of more intensive ionization. Then, a higher electric field is created near the arc spot although the area intensively concentrates near the arc spot.

Accordingly, the experimental results shown in Section 4 can be explained from the calculated ones. The arcing characteristics strongly depend on characteristics of ambient plasma, specially neutral particle number density. Therefore, both the properties of spacecraft insulator materials and the characteristics of ambient plasmas around spacecraft are key factors to determine arcing phenomena on spacecraft surface insulators.

Conclusions

Ground-based experiment was carried out to understand discharge phenomena on spacecraft surface and to examine influences of ambient space plasma on the arcing process. Simulating plasmas were generated by electron cyclotron resonance discharge. The measured arcing characteristics for negatively-biased anodized aluminum sample (AAS) plates in the plasma environment showed that both the peak arc current and the total charge emitted by arcing increased with initial charging voltage and neutral particle number density. The diameter of arc spots increased with initial charging voltage although it was almost constant regardless of neutral particle density. Furthermore, Direct-Simulation-Monte-Carlo Particle-In-Cell plasma simulation was conducted to understand features of plasma expanding from an arc spot on spacecraft surface into the ambient plasma just after arcing. The calculated results showed that neutral particles in addition to charged particles around spacecraft played an important role in expansion of arc plasma causing the arcing characteristics. Accordingly, high voltage operation of LEO spacecraft might bring drastic degradation of AAS by arcing; particularly with high neutral particle density, a high arc current is suspected to flow.

References

1. NASA/SDIO Space Environmental Effects on Material Workshop, NASA CP-3035, 1989.

2. H. Tahara, L. Zhang, M. Hiramatsu, T. Yasui, T. Yoshikawa, Y. Setsuhara and S. Miyake," Exposure of Space Material Insulators to Energetic Ions," J. Appl. Phys., Vol.78, No.6, pp.3719-3723, 1995.

3. L. Zhang, T. Yasui, H. Tahara and T. Yoshikawa," X-ray Photoelectron Spectroscopy Study of the Interactions of O^+ and N^+ Ions with Polyimide Films," Jpn. J. Appl. Phys., Vol.36, No.8, pp.5268-5274, 1997.

4. A.C. Tribble, R. Lukins, E. Watts, V.A. Borisov, S.A. Demidov, V.A. Denisenko, A.A. Gorodetskiy, V.K. Grishin, S.F. Nauma, V.K. Sergeev and S.P. Sokolova," United States and Russian Thermal Control Coating Results in Low Earth Orbit," J. Spacecraft & Rockets, Vol.33, No.1, pp.160-166, 1996.

5. H. Tahara, K. Kawabata, L. Zhang, T. Yasui and T. Yoshikawa," Exposure of Spacecraft Polymers to Energetic Ions, Electrons and Ultraviolet Light," Nucl. Instrum. & Methods, Vol.B121, pp.446-449, 1997.

6. D. Matsuyama, H. Tahara, T. Matsuda, T. Yasui and T. Yoshikawa," Ground Experiments of Interaction between Plasma Flow and Negatively Biased or Charged Materials," Proc. 26th Int. Electric Propulsion Conf., Kitakyushu, Japan, IEPC-99-224, pp.1314-1321, 1999.

7. H. Tahara, T. Yasui, D. Matsuyama and T. Yoshikawa," Laboratory Simulation of Charging Relaxation by Plasma Flow," Proc. 7th Spacecraft Charging Technology Conf., ESTEC, Noordwijk, The Netherlands, ESA SP-476, 2001.

8. H. Tahara, D. Matsuyama, T. Yasui and T. Yoshikawa," Mitigation Process of Spacecraft Negative Charging by Plasma Flow," 27th Int. Electric Propulsion Conf., Pasadena, CA, USA, IEPC-01-258, 2001.

9. H. Tahara, T. Yasui and T. Yoshikawa," Space Plasma Simulator Performance Using an Electron Cyclotron Resonance Plasma Accelerator," Trans. Japan Soc. Aero. Space Sci., Vol.40, No.127, pp.59-68, 1997.